Electronic Supporting Information

Calix[6]arene-Functionalized Titanium-oxo clusters for Photocatalytic Cycloaddition of Carbon Dioxide to Epoxides

Jinle Hou,*[a] Yuxin Liu,[a] Nahui Huang,[a] Mohammad Azam,[c] Chen Huang,[a] Zhi Wang,[b] Xianqiang Huang,*[a] Konggang Qu[a] and Di Sun*[b]

[a] Shandong Provincial Key Laboratory of Chemical Energy Storage and Novel Cell Technology, and School of Chemistry and Chemical Engineering, Liaocheng University, Liaocheng, 252000, People's Republic of China. E-mail: houjinle@lcu.edu.cn (J. L. Hou); hxq@lcu.edu.cn (X. Q. Huang).

[b] School of Chemistry and Chemical Engineering, Shandong University, Jinan, 250100, People's Republic of China. E-mail: dsun@sdu.edu.cn (D. Sun).

[c] Department of Chemistry, College of Science, King Saud University, PO BOX 2455 Riyadh, 11451, Saudi Arabia.

Experimental Procedures

Materials and Instruments

Titanium (IV) tetraisopropanolate ($Ti(^{i}PrO)_{4,}$ 98%, Adamas-beta®) was purchased from Shanghai Titan Scientific Co., Ltd. Tert-butylcalix[6]arene (TBC6A) was purchased from Shanghai Macklin Biochemical Technology Co., Ltd. Acetonitrile (CH_3CN), malonic acid (MA), chlorobenzene, propionic acid (PA), dichloromethane, series of epoxy compounds, and tetrabutylammonium bromide (TBAB) were purchased from Sinopharm Chemical Reagent Co., Ltd, China. All chemicals and solvents were analytical grade and used without further purification. Powder X-ray diffraction (PXRD) data were carried out on a microcrystalline powdered sample using a Rigaku SmartLab-9Kw diffractometer using Cu radiation (λ = 1.54184 Å). Thermogravimetry (TG) analysis was performed on a STA449F5/QMS403D instrument (Mettler-Toledo, Schwerzenbach, Switzerland) with a heating rate of 10 °C min^{-1} from 20 to 800 °C in N_2 flow. The solid-state UV/Vis spectra data of the cluster samples were obtained using a Carry 500 UV-VIS spectrophotometer with scanning wavelength range from 200 nm to 800 nm. Fourier transform infrared spectroscopy (FTIR) measurements were obtained using a Nicolet iS50 spectrophotometer. The X-ray photoelectron spectroscopy (XPS) spectra were collected on a Thermo Scientific ESCALAB Xi^{+} instrument. The high-resolution electrospray ionization mass spectrometry (ESI-MS) of **Ti28-TBC6A** were acquired on an ACQUITY UPLC I-Class/Xevo G2-XS QTOF (Waters, Milford, USA) mass spectrometer. The data analysis of the mass spectrum was performed based on the isotope distribution patterns using MassLynx Analysis software (Version 4.1). The element mapping of samples were acquired on a Thermo Fisher Scientific FIB-SEM-GX4 scanning electron microscope. Electrochemical measurements were carried out on a CHI 660E electrochemical workstation. Gas chromatographic (GC) analysis was carried out on a Shimadzu GC-2014C instrument equipped with a flame ionization detector (FID). Gas chromatogram and mass spectrum authentication were performed on an Agilent 7000D.

Synthesis

Synthesis of $[Ti_4(\mu_3\text{-}O)_2(TBC6A)_2(CH_3CN)_2]\cdot CH_3CN$ (Ti4-TBC6A)

0.73 mmol (10 mg) of TBC6A and 1 mmol (104 mg) of malonic acid were ultrasonically dissolved in 5 mL of acetonitrile. 0.33 mmol (0.1 mL) of $Ti(^iPrO)_4$ was then added. The mixture was sealed in a 10 mL glass vial and heated at 100 °C for 72 hours. After cooling to room temperature, yellow crystals were obtained by filtration and washed several times with ethanol. The yield of **Ti4-TBC6A** was 23% (based on $Ti(^iPrO)_4$).

Synthesis of $[Ti_{28}(\mu_2\text{-}O)_{18}(\mu_3\text{-}O)_{18}(TBC6A)(PA)_{34}(^iPrO)_2]\cdot 4CH_3CN$ (Ti28-TBC6A)

Similar to **Ti4-TBC6A**, except the 1 mmol (104 mg) of malonic acid was replaced with propionic acid (0.5 mL). The other conditions were kept the same. After cooling to room temperature, brown crystals were obtained by filtration and washed several times with ethanol. The yield of **Ti28-TBC6A** was 17% (based on $Ti(^iPrO)_4$).

Single-crystal X-ray diffraction

Single crystals of **Ti4-TBC6A** and **Ti28-TBC6A** were selected under an optical microscope and rapidly coated with high vacuum grease (Dow Corning Corporation) to prevent decomposition. The single-crystal diffraction analysis of **Ti4-TBC6A** and **Ti28-TBC6A** were recorded on Bruker D8 VENTURE diffractometer with an Incoatec IμS 3.0 Cu EF (Incoatec IμS diamond Mo) microfocus source (55W, Cu Kα, λ = 1.54184 Å) at 173 K equipped with a PHOTON III C28 detector and an Oxford Cryosystems CryostreamPlus 800 open-fow N_2 cooling device. These structures were solved by the inherent phase method in the SHELXT program and refined by full-matrix least squares techniques against F^2 using the SHELXL program through the OLEX2 interface. Hydrogen atoms at carbon were placed in calculated positions and refined isotropically by using a riding model. Appropriate restraints or constraints were applied to the geometry and the atomic displacement parameters of the atoms in the cluster. All structures were examined using the Addsym subroutine of PLATON to ensure that no additional symmetry could be applied to the models. Pertinent crystallographic data collection and refinement parameters are collated in Table S2. Selected bond lengths are collated in Table S3. The crystallographic data for **Ti4-TBC6A** and **Ti28-TBC6A** were delivered to the Cambridge Crystallographic Data Centre (CCDC) with *No.* 2344847 for **Ti4-TBC6A** and 2344848 for **Ti28-TBC6A**. These data can be obtained from the CCDC via www.ccdc.cam.ac.uk/data_request/cif.

Electrochemical measurements

Photoelectrochemical measurements

Photoelectrochemical measurements were carried out on CHI 660E electrochemical workstation in a standard three-electrode electrochemical cell with ITO coated with the crystals as the working electrode, a platinum plate as counter electrode and a saturated Ag/AgCl electrode as reference electrode. A sodium sulfate solution (0.2 M) was used as the electrolyte, and a Xe lamp (150 W) was used as the light source. A bias potential of 0.4 V was maintained. Preparation of the working electrode: 2 mg crystals powder was mixed with 0.99 mL ethanol and 10 μL Nafion D-520 dispersion solutions and sonicated for 30 minutes. Subsequently, 200 μL of slurry was transferred, coated on ITO glass plates (1 cm×2 cm), and then dried at room temperature.

Electrochemical impedance spectroscopy

Electrochemical impedance spectra (EIS) measurements were also carried out on CHI 660E electrochemical workstation via a conventional three-electrode system with a working electrode, a platinum plate as counter electrode and a saturated Ag/AgCl electrode as reference electrode in a 0.2 M Na_2SO_4 aqueous solution over a frequency range of 100 kHz-0.01 Hz.

Computational Studies

The geometric structure of **Ti4-TBC6A** and **Ti28-TBC6A** are optimized by using Perdew-Burke-Ernzerhof (PBE) exchange-correlation functional in DMol^3.[1–3] The DFT-based relativistic semi-core pseudopotential (DSPP) and double numerical plus *d*-functions (DND) basis sets were used to calculate the energy of structural. The convergence criterion of the geometric optimization and electronic structure calculation was set to be 1.0×10^{-5} Hartree for energy change, 2.0×10^{-3} Hartree/Å for the gradient, and 3.0×10^{-3} Å for the displacement, respectively. Dispersion corrections in Grimme's scheme (DFT-D3) was applied to treat the long-range van der Waals interactions.[4]

General Procedure for Photocatalytic Reactions

In a typical experiment, 15 mg of **Ti4-TBC6A** or **Ti28-TBC6A**, 0.30 mmol of tetrabutylammonium bromide (TBAB), and 200 μL of chlorobenzene were added into a 20 mL vial. The vial was sealed with a rubber stopper and purged with CO_2 for approximately 5 minutes. Subsequently, 4.0 mmol of epoxide was added using a microsyringe. Then, at room temperature, the experiment was conducted in a Wattecs Parallel Photocatalytic Reactor (WP-TEC-1020HSL) under a CO_2 atmosphere (1 atm., balloon), using a 10 W 430 nm LED (Xi'an Wattecs Experimental Equipment Co., LTD., China) for irradiation. Simultaneously, it was stirred at 500 rpm for an appropriate reaction time. During the reaction, a water bath was used to maintain the temperature nearly constant at 293 K. After a certain time, an aliquot of the solution sample was extracted quantitatively using ethyl acetate and water (1:1 v/v). Chlorobenzene was used as an internal standard, and the epoxide compounds and cyclocarbonate products were quantified using GC (Shimadzu GC-2014C).

Figure S1. The compared PXRD patterns of **Ti4-TBC6A**.

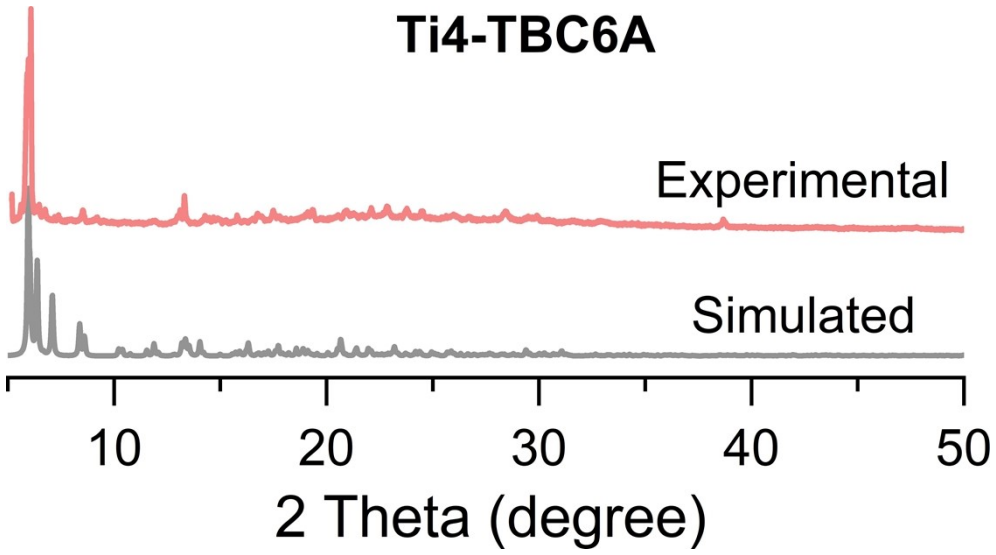

Figure S2. The compared PXRD patterns of **Ti28-TBC6A**.

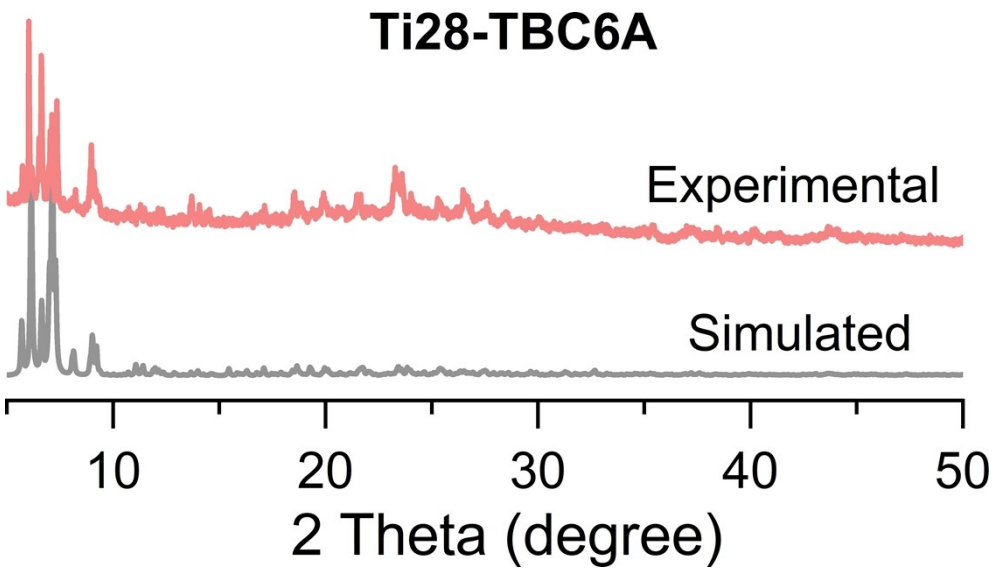

Figure S3. The thermogravimetric analysis (TGA) curves of **Ti4-TBC6A** and **Ti28-TBC6A**.

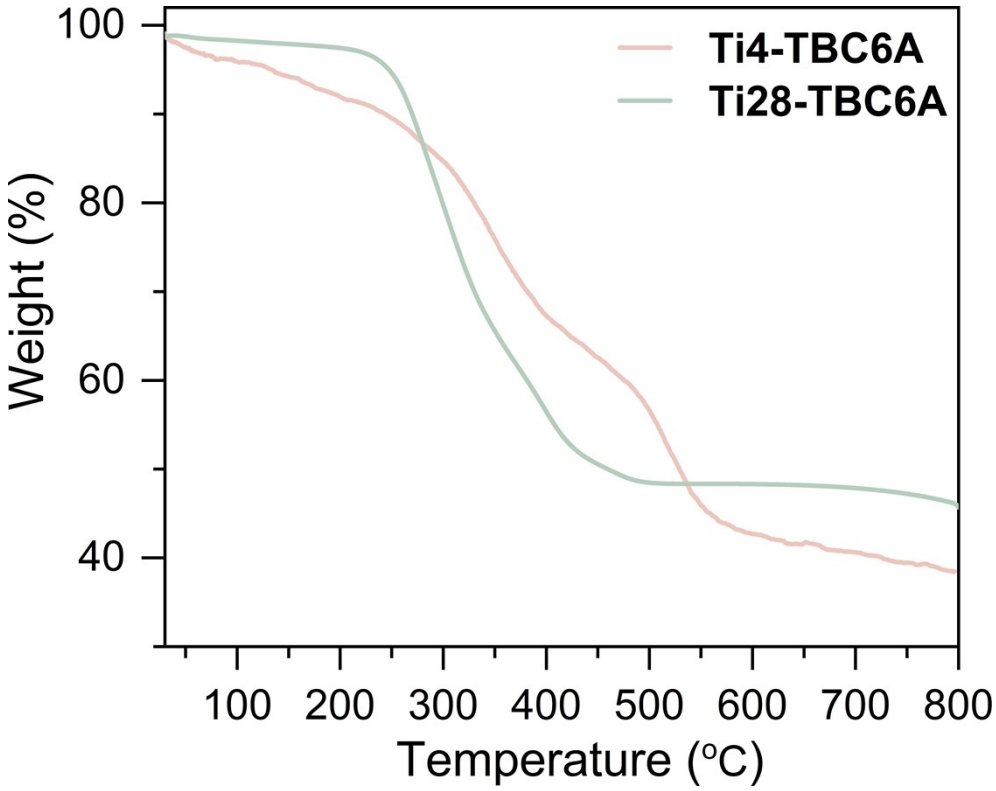

Figure S4. The Fourier transform infrared spectroscopy (FT-IR) of TBC6A, **Ti4-TBC6A** and **Ti28-TBC6A**.

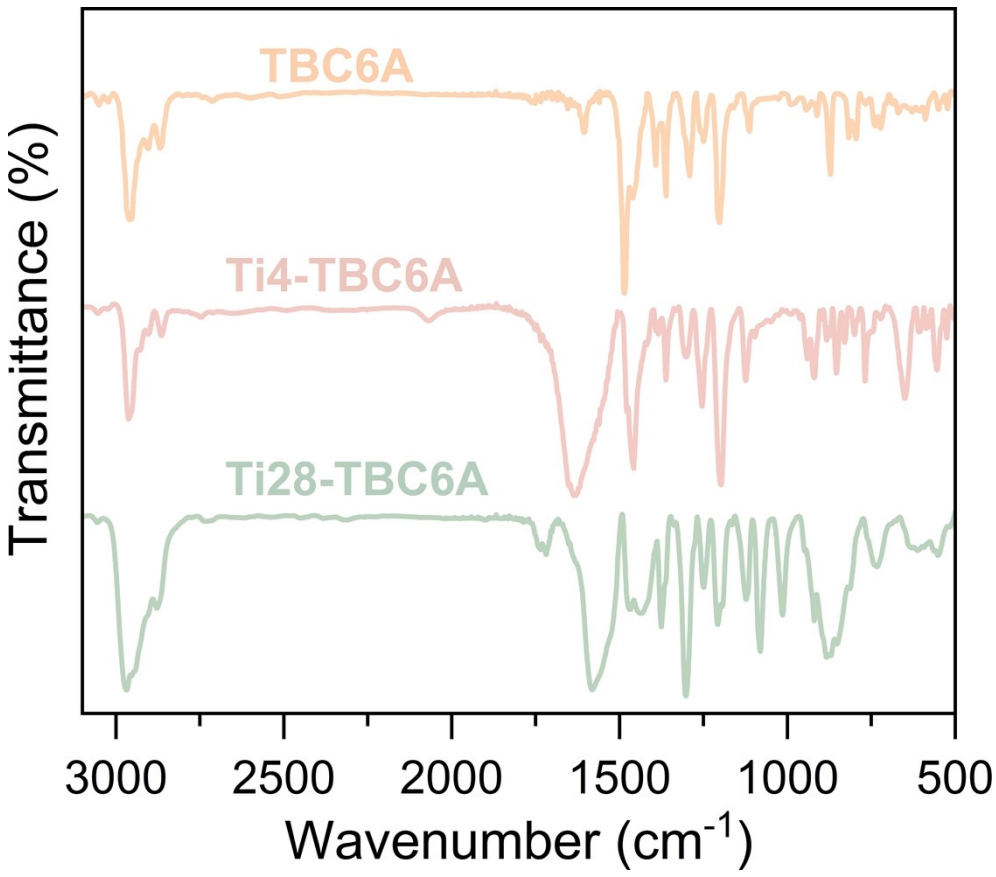

Figure S5. Elemental mapping images of Ti, O and C of selected area for **Ti4-TBC6A**.

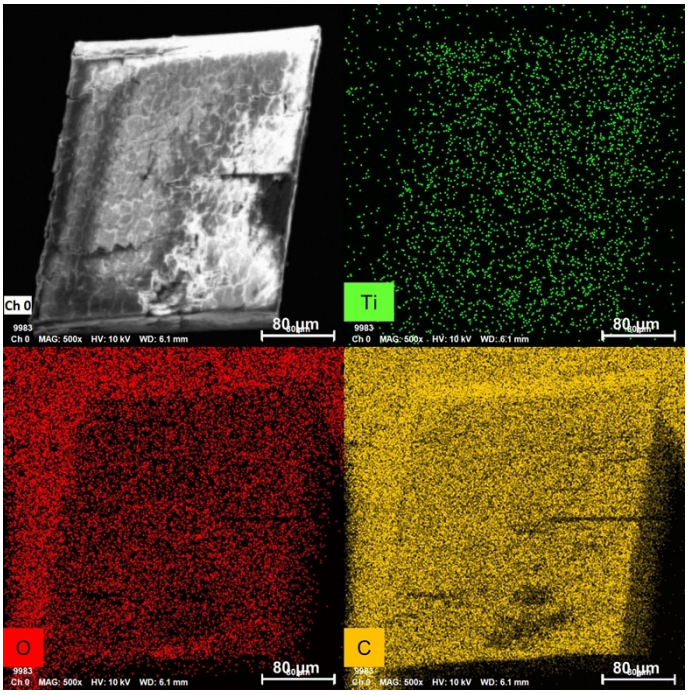

Figure S6. Elemental mapping images of Ti, O and C of selected area for **Ti28-TBC6A**.

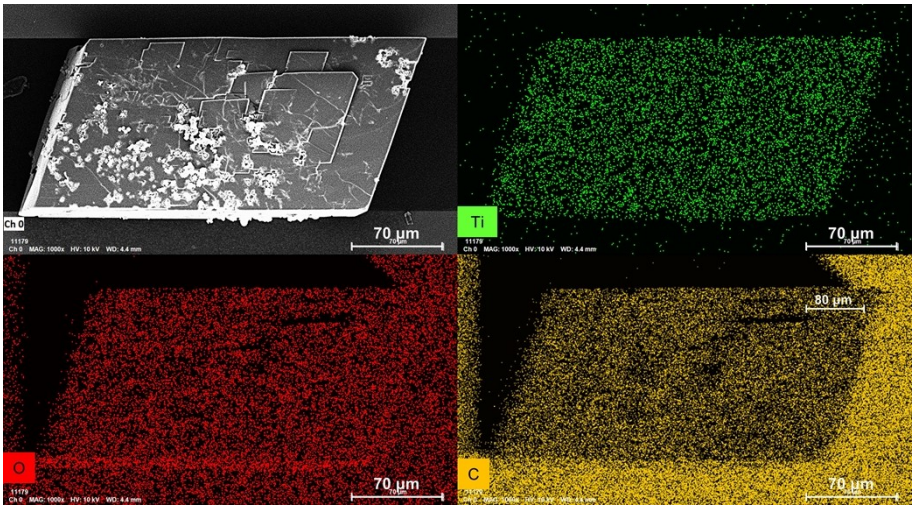

Figure S7. X-ray photoelectron spectroscopy (XPS) spectra of (a, b) **Ti4-TBC6A** and (c, d) **Ti28-TBC6A**. XPS results reveal that all Ti atoms in **Ti4-TBC6A** and **Ti28-TBC6A** are exclusively in the +4 oxidation state.

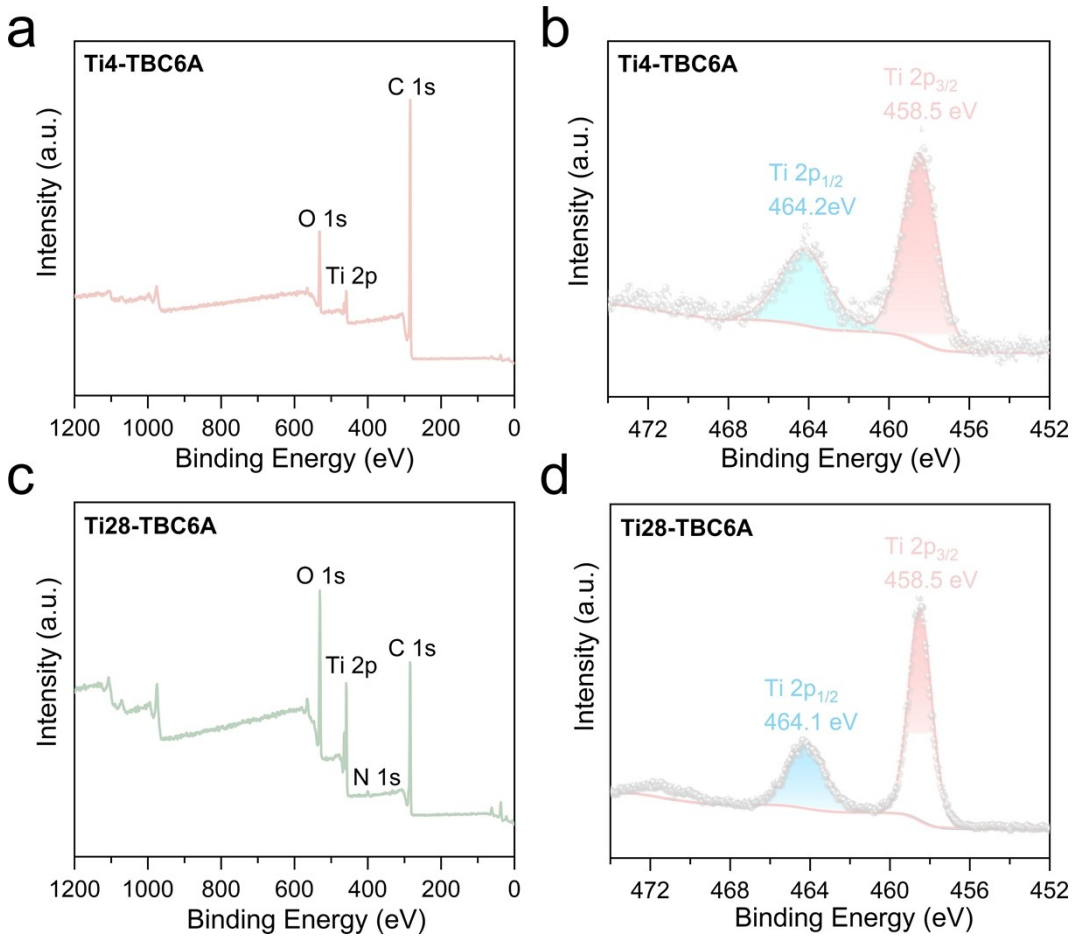

Figure S8. (a) The asymmetric unit of **Ti4-TBC6A**. Molecule packing diagrams in a 1×1×1 unit cell of **Ti4-TBC6A** viewed along the *a* (b), *b* (c), and *c* (d) axis.

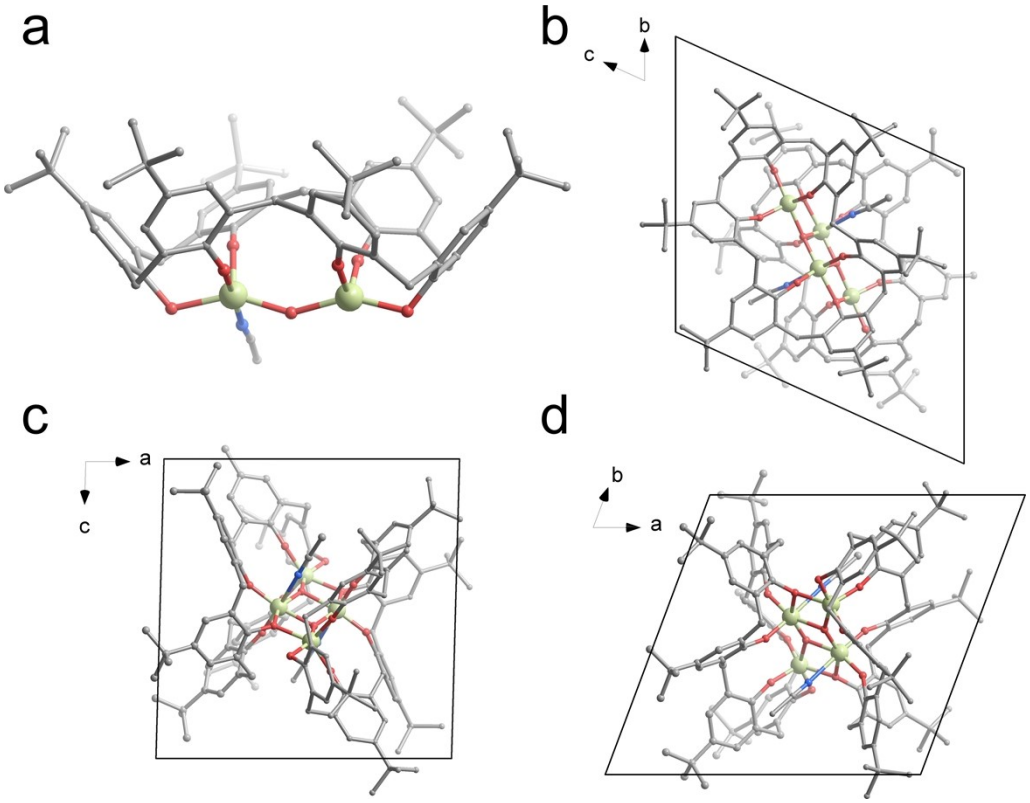

Figure S9. (a) The coordination mode of TBC6A in **Ti4-TBC6A**. (b) Surface ligand distribution of {Ti_{14}} subunit, where pink represents acetate ligands and cornsilk represents isopropanol. (c) The coordination mode of TBC6A in **Ti28-TBC6A**.

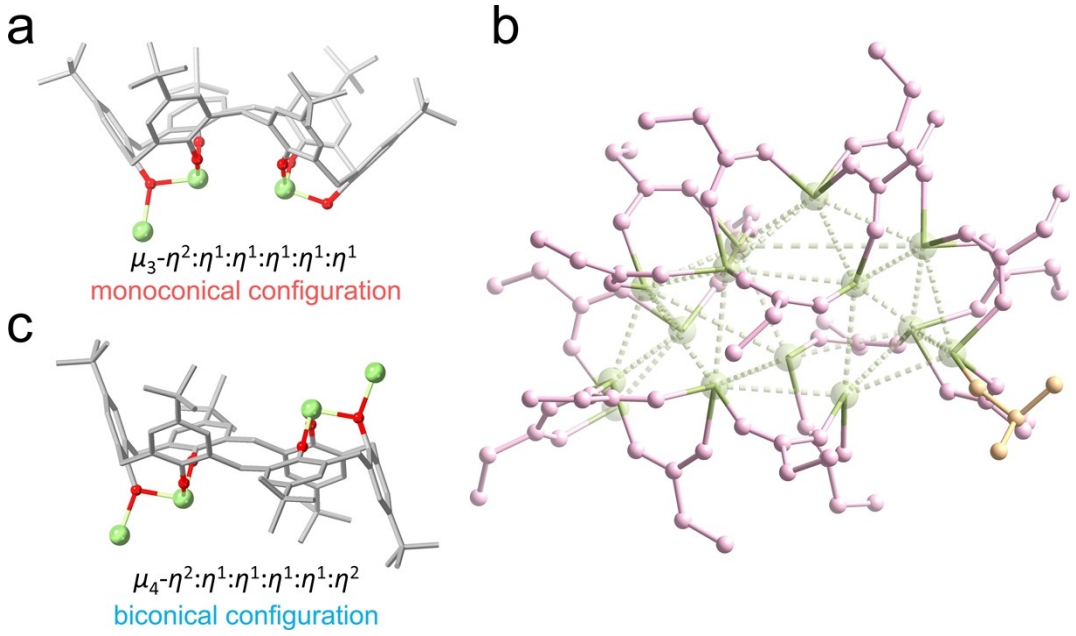

Figure S10. (a) The asymmetric unit of **Ti28-TBC6A**. Molecule packing diagrams in a 1×1×1 unit cell of **Ti28-TBC6A** viewed along the *a* (b), *c* (c), and *b* (d) axis.

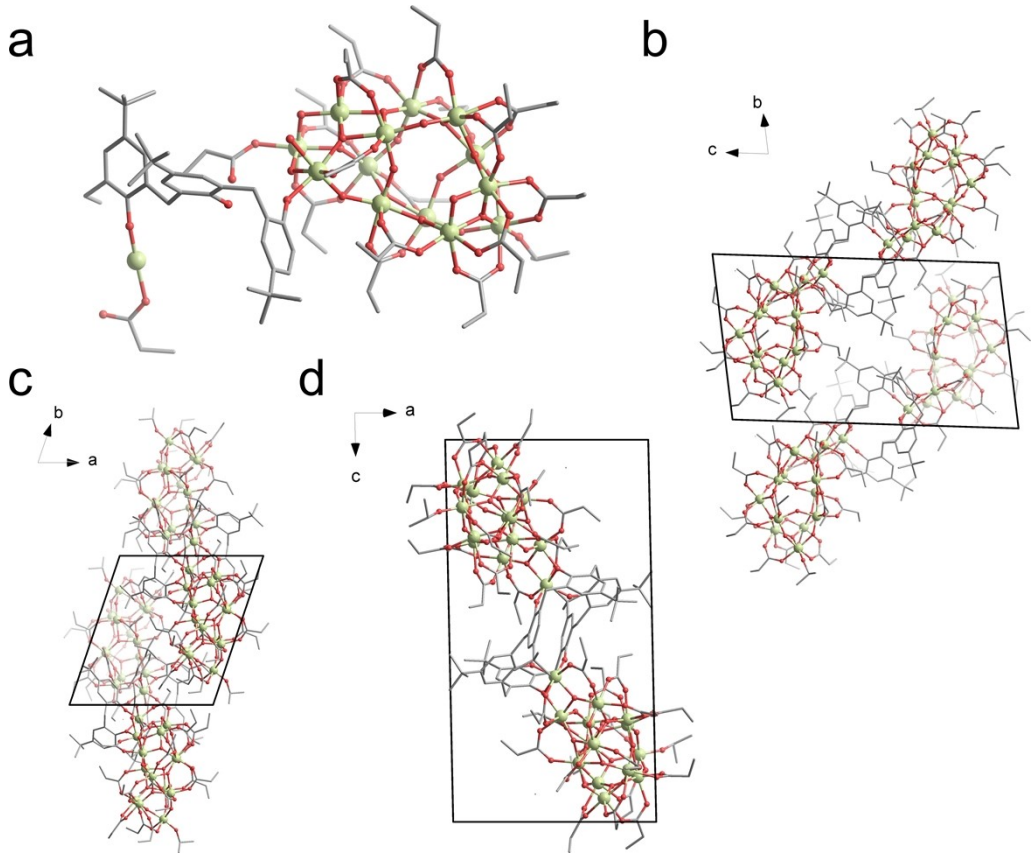

Figure S11. The images of **Ti4-TBC6A** and **Ti28-TBC6A** under optical microscope.

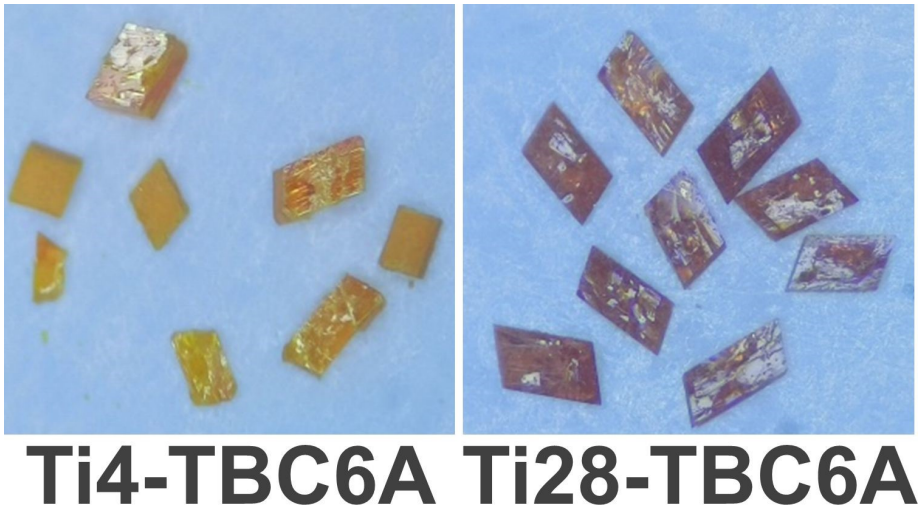

Figure S12. Tauc plots of TBC6A, **Ti4-TBC6A** and **Ti28-TBC6A**.

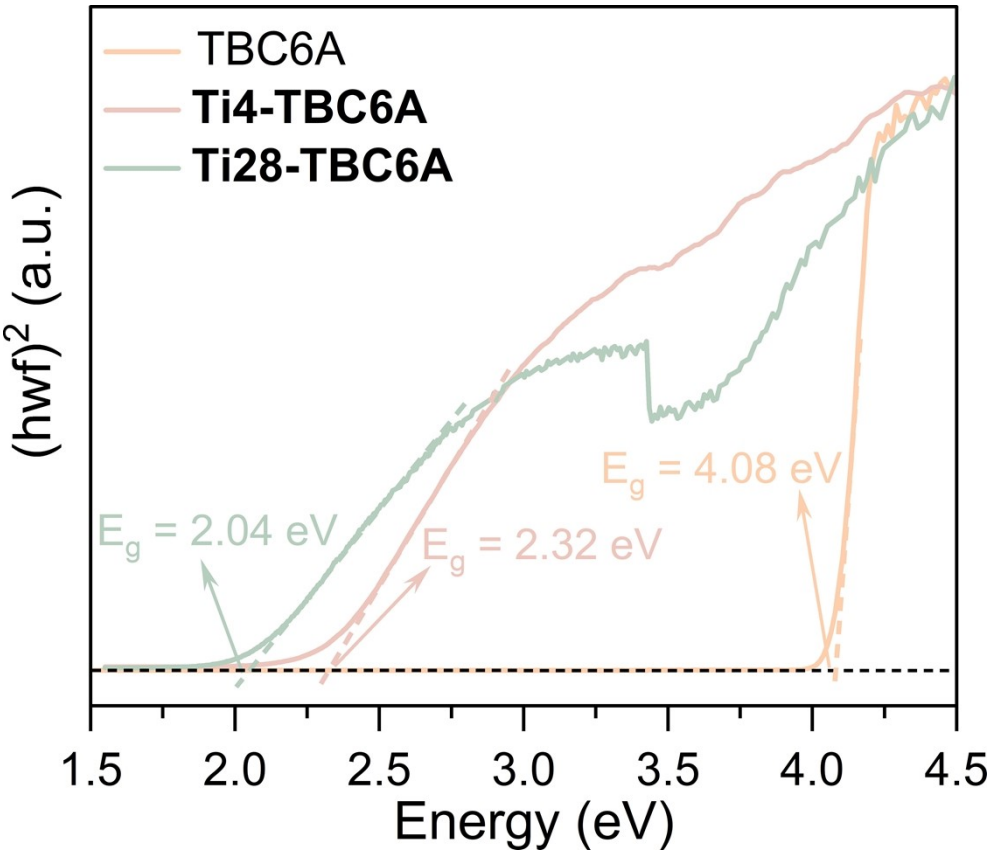

Figure S13. Molecular orbital distribution of selected HOMOs and LUMOs for **Ti4-TBC6A** based on DFT calculations.

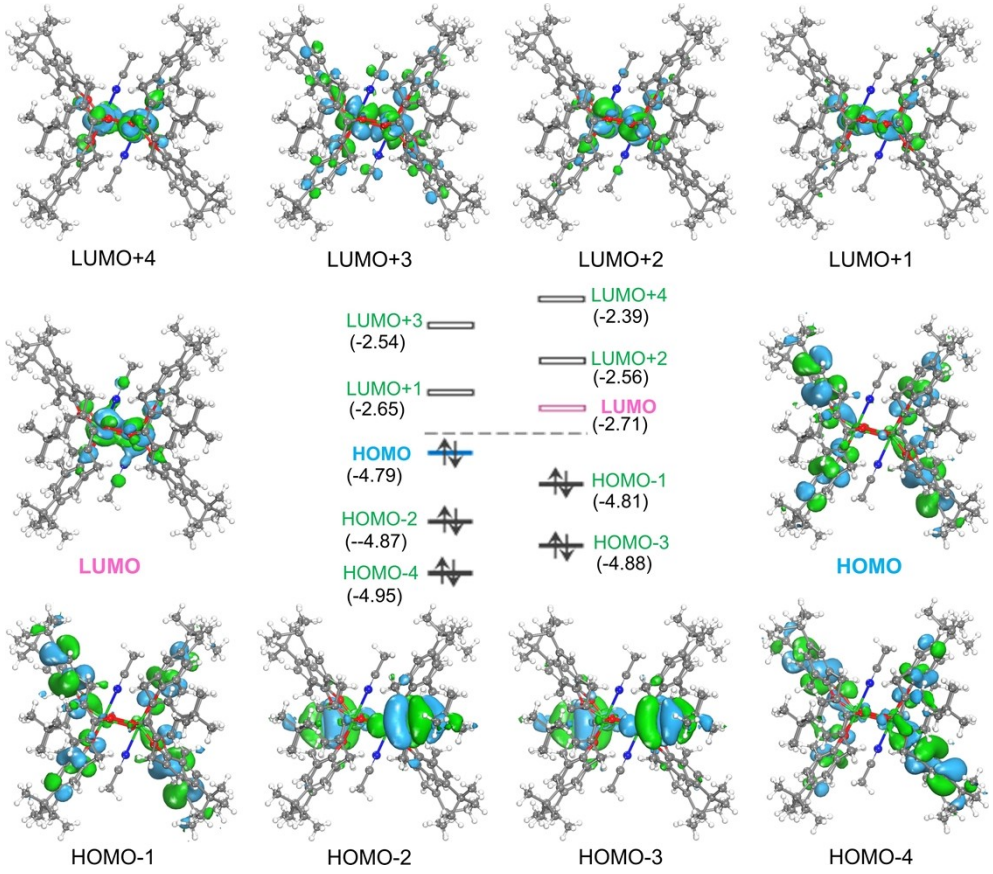

Figure S14. Positive-ion mode ESI-MS of the system before and after the reaction of photocatalytic cycloaddition of CO_2 and epoxides, using **Ti28-TBC6A** as the photocatalyst and diluted with CH_2Cl_2. Insets display the experimental (purple) and simulated (red) isotopic distribution patterns for species **1a**.

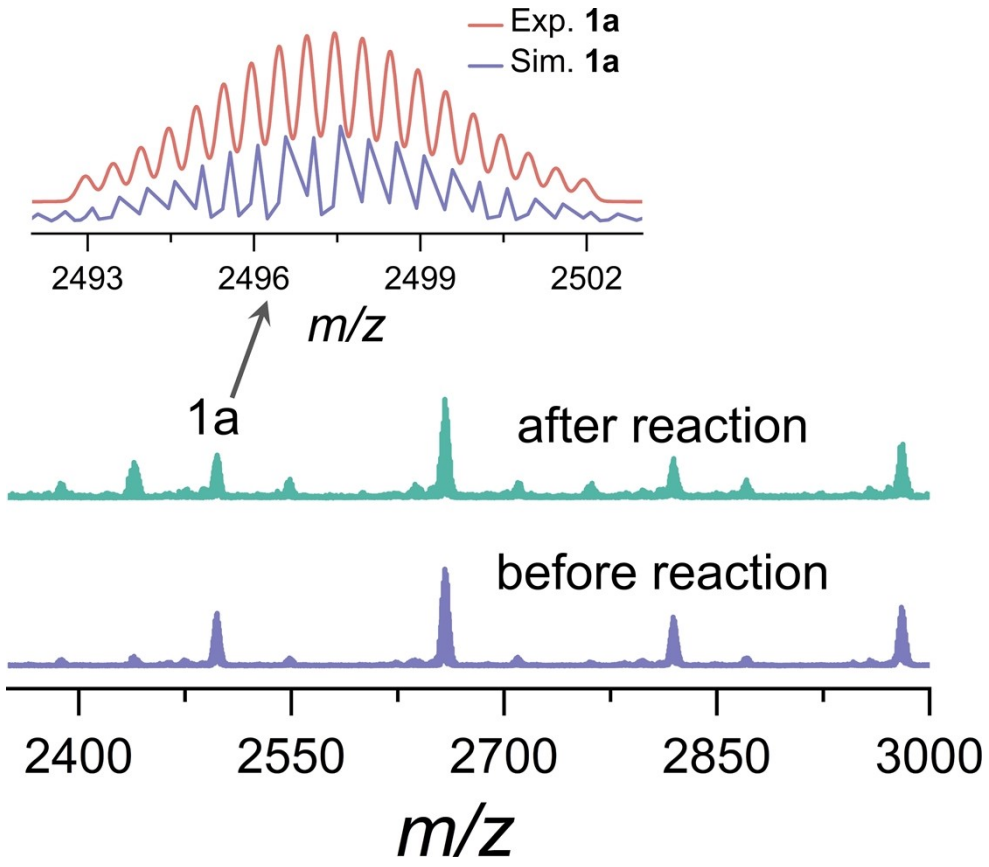

Figure S15. The GC and GC-MS analysis of the cycloaddition reaction of CO_2 and styrene oxide after 20 h over the **Ti28-TBC6A** photocatalyst.

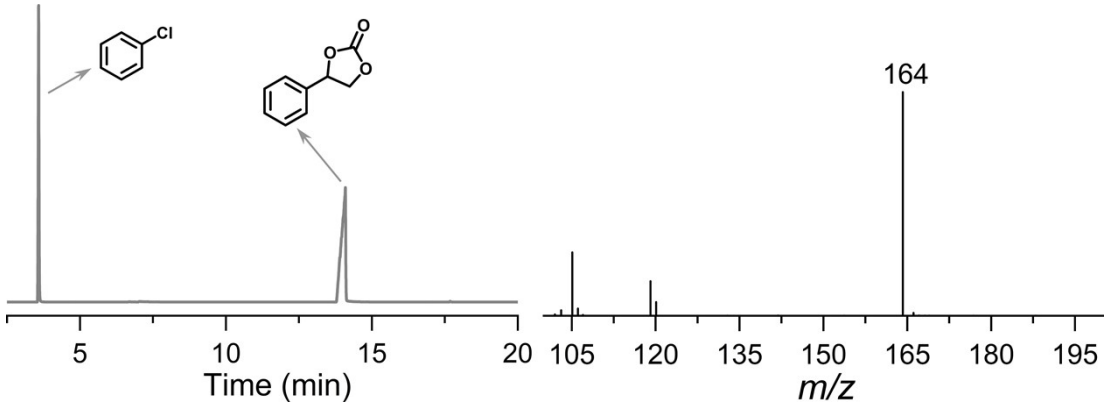

Figure S16. The GC and GC-MS analysis of the cycloaddition reaction of CO_2 and glycidyl phenyl ether after 20 h over the **Ti28-TBC6A** photocatalyst.

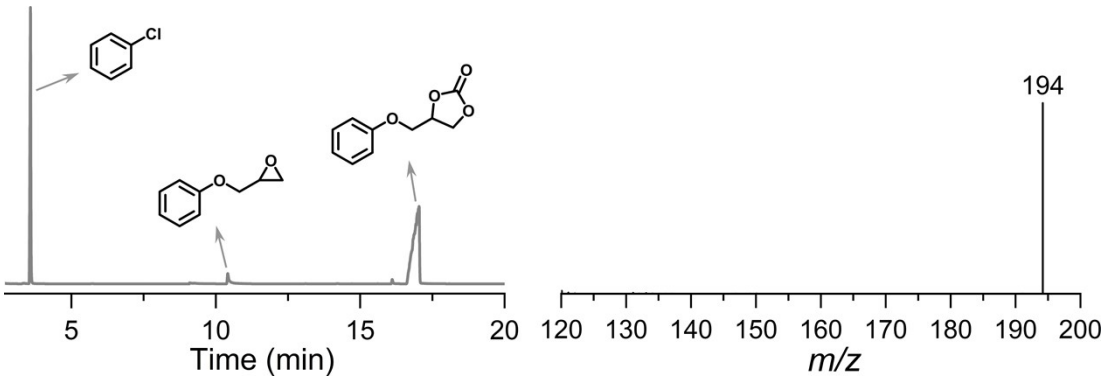

Figure S17. The GC and GC-MS analysis of the cycloaddition reaction of CO_2 and benzyl glycidyl ether after 20 h over the **Ti28-TBC6A** photocatalyst.

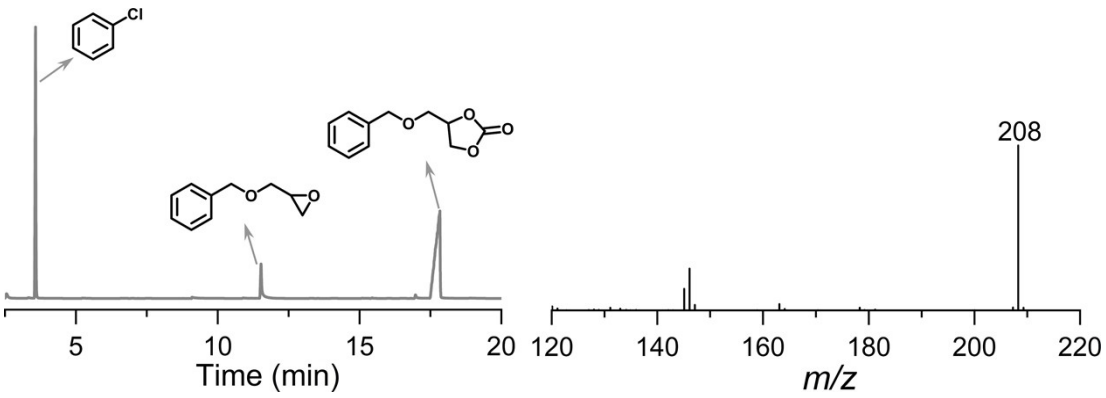

Figure S18. The GC and GC-MS analysis of the cycloaddition reaction of CO_2 and epichlorhydrin after 20 h over the **Ti28-TBC6A** photocatalyst.

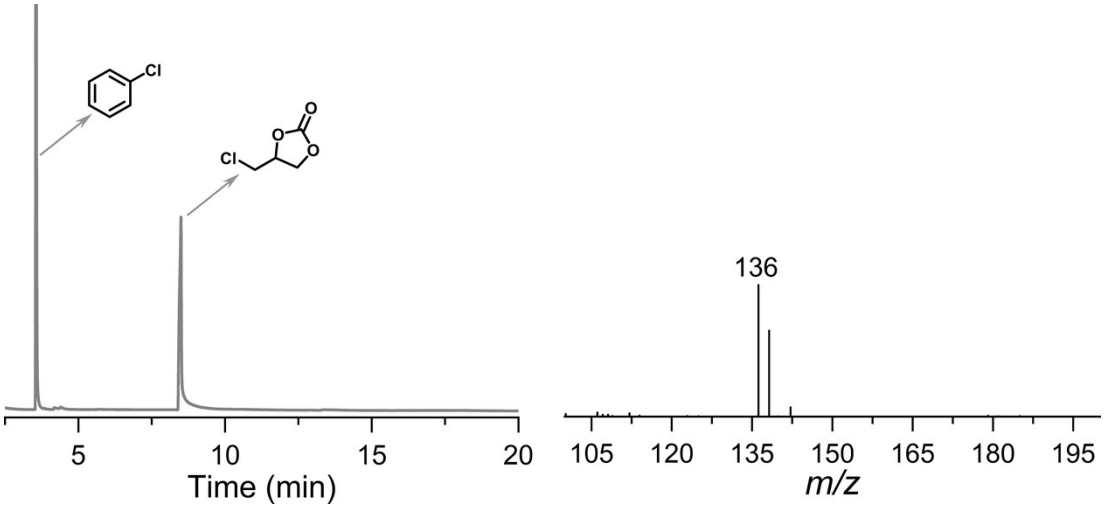

Figure S19. The GC and GC-MS analysis of the cycloaddition reaction of CO_2 and epibromohydrin after 20 h over the **Ti28-TBC6A** photocatalyst.

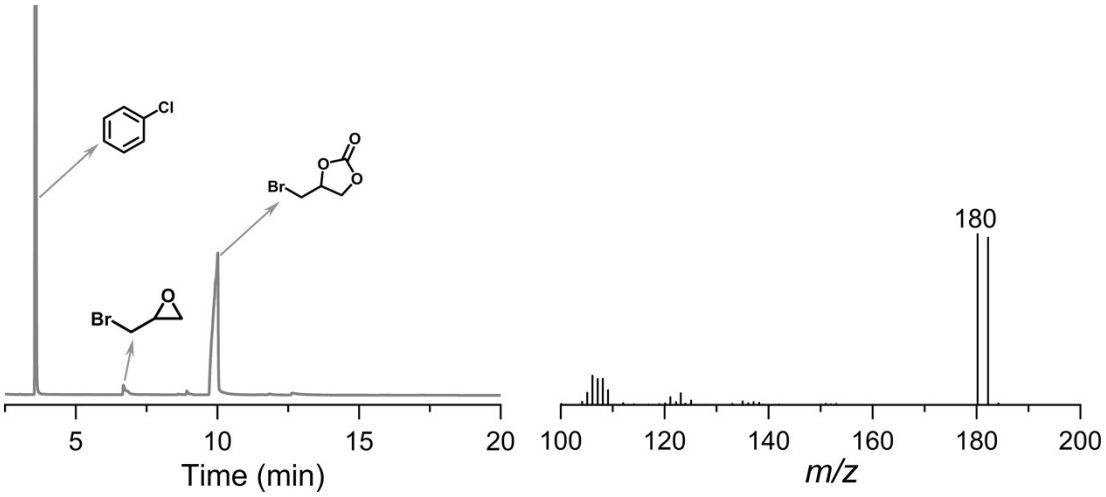

Figure S20. The GC and GC-MS analysis of the cycloaddition reaction of CO_2 and 1,2-epoxyoctane after 20 h over the **Ti28-TBC6A** photocatalyst.

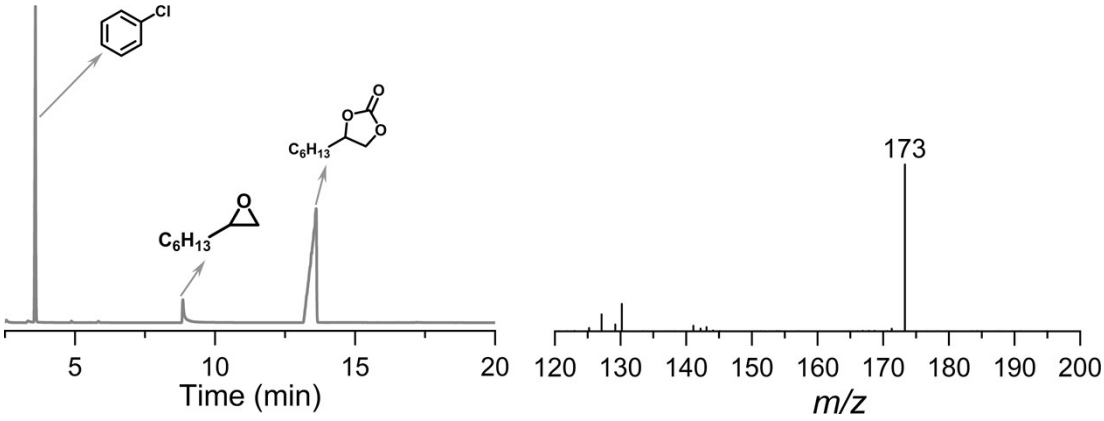

Figure S21. The GC and GC-MS analysis of the cycloaddition reaction of CO_2 and allyl glycidyl ether after 20 h over the **Ti28-TBC6A** photocatalyst.

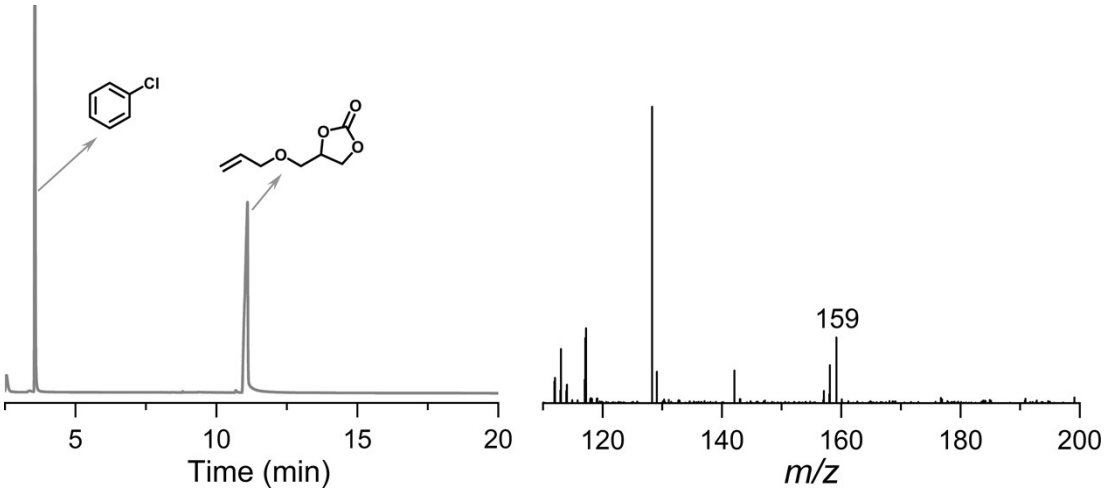

Table S1. Bond valence sum (BVS) analysis[a] for **Ti4-TBC6A** and **Ti28-TBC6A**.

Ti4-TBC6A					
Ti1 4.374			**Ti2 4.211**		
Ti1–O1$^{\#1}$	d=2.017	0.579	Ti2–O1	d=1.943	0.708
Ti1–O1	d=1.894	0.808	Ti2–O2	d=1.809	1.016
Ti1–O4	d=1.821	0.983	Ti2–O3	d=1.877	0.847
Ti1–O5	d=1.996	0.613	Ti2–O5$^{\#1}$	d=2.048	0.533
Ti1–O6	d=1.805	1.027	Ti2–O7	d=1.777	1.107
Ti1–N1	d=2.304	0.364			

Continued above

Ti28-TBC6A								
Ti1 4.175			**Ti2 4.163**			**Ti3 4.138**		
Ti1–O37	d=1.938	0.717	Ti2–O37	d=1.902	0.791	Ti3–O51	d=2.024	0.569
Ti1–O2	d=2.019	0.576	Ti2–O40	d=1.973	0.653	Ti3–O40	d=2.052	0.526
Ti1–O39	d=1.929	0.735	Ti2–O41	d=1.809	1.016	Ti3–O41	d=1.829	0.964
Ti1–O5$^{\#1}$	d=2.125	0.432	Ti2–O7	d=1.997	0.612	Ti3–O39	d=1.878	0.844
Ti1–O38	d=1.770	1.128	Ti2–O10	d=2.028	0.563	Ti3–O35	d=1.984	0.633
Ti1–O20	d=2.012	0.587	Ti2–O8	d=2.050	0.530	Ti3–O33	d=2.003	0.601
Ti4 4.123			**Ti5 4.186**			**Ti6 4.166**		
Ti4–O42	d=1.889	0.819	Ti5–O42	d=1.900	0.795	Ti6–O51	d=1.977	0.646
Ti4–O40	d=1.890	0.815	Ti5–O43	d=2.023	0.570	Ti6–O39	d=2.045	0.538
Ti4–O52	d=1.840	0.935	Ti5–O53	d=1.838	0.940	Ti6–O21	d=2.017	0.579
Ti4–O11	d=2.069	0.503	Ti5–O38	d=1.854	0.900	Ti6–O53	d=1.776	1.112
Ti4–O12	d=2.055	0.523	Ti5–O17	d=2.099	0.464	Ti6–O45	d=1.866	0.871
Ti4–O9	d=2.051	0.529	Ti5–O18	d=2.059	0.517	Ti6–O34	d=2.135	0.421
Ti7 4.170			**Ti8 4.155**			**Ti9 4.106**		
Ti7–O42	d=2.217	0.337	Ti8–O51	d=1.914	0.764	Ti9–O54	d=1.965	0.667
Ti7–O43	d=1.944	0.705	Ti8–O52	d=1.830	0.960	Ti9–O55	d=1.960	0.676
Ti7–O55	d=1.974	0.652	Ti8–O58	d=1.858	0.890	Ti9–O56	d=1.743	1.214
Ti7–O44	d=1.726	1.270	Ti8–O14	d=2.057	0.520	Ti9–O58	d=2.169	0.384
Ti7–O16	d=2.013	0.585	Ti8–O32	d=2.058	0.519	Ti9–O29	d=2.015	0.583
Ti7–O13	d=1.991	0.622	Ti8–O31	d=2.070	0.501	Ti9–O15	d=2.015	0.582
Ti10 4.154			**Ti11 4.155**			**Ti12 4.149**		
Ti10–O54	d=1.989	0.625	Ti11–O43	d=1.885	0.827	Ti12–O54	d=1.920	0.753
Ti10–O45	d=1.764	1.148	Ti11–O46	d=1.899	0.798	Ti12–O46	d=1.895	0.806
Ti10–O58	d=1.906	0.781	Ti11–O47	d=1.848	0.916	Ti12–O47	d=1.809	1.017
Ti10–O28	d=2.129	0.428	Ti11–O24	d=2.089	0.477	Ti12–O25	d=2.047	0.534
Ti10–O30	d=2.015	0.582	Ti11–O19	d=2.013	0.586	Ti12–O26	d=2.072	0.500
Ti10–O57	d=2.010	0.590	Ti11–O22	d=2.035	0.552	Ti12–O48	d=2.043	0.539
Ti13 4.225			**Ti14 4.227**					
Ti13–O56	d=1.920	0.752	Ti14–O37$^{\#1}$	d=2.016	0.581			
Ti13–O46	d=2.049	0.531	Ti14–O2$^{\#1}$	d=2.012	0.587			
Ti13–O44	d=1.918	0.758	Ti14–O1$^{\#1}$	d=1.828	0.965			
Ti13–O23	d=2.052	0.527	Ti14–O6$^{\#1}$	d=2.019	0.576			
Ti13–O36	d=1.771	1.125	Ti14–O3	d=1.802	1.037			
Ti13–O27	d=2.049	0.532	Ti14–O4	d=2.084	0.483			

[a] $V_i = \Sigma S_{ij} = \Sigma \exp[(r_1 - r_{ij})/B]$, where r_{ij} is the bond length between atoms i and j (with r_1 = 1.791 for Ti^{iv}-O and 1.906 for Ti^{iv}-N). The constant B is approximately equal to 0.37 Å. S_{ij} is the valence of a bond between atoms i and j, and V_i is the sum of all bond valences of the bonds formed by a given atom.[5]

Table S2. Crystal data collection and sructure refinement for **Ti4-TBC6A** and **Ti28-TBC6A**.

Compound	**Ti4-TBC6A**	**Ti28-TBC6A**
Empirical formula	$C_{148}H_{180}N_8O_{14}Ti_4$	$C_{182}H_{274}N_4O_{112}Ti_{28}$
Formula weight	2486.59	5651.24
Temperature [K]	173.0	173.0
Crystal system	triclinic	triclinic
Space group (number)	$P\bar{1}$ (2)	$P\bar{1}$ (2)
a [Å]	15.7410(11)	14.9596(5)
b [Å]	16.4017(12)	16.5694(6)
c [Å]	16.4595(12)	26.9838(6)
α [°]	64.279(3)	80.4020(10)
β [°]	81.984(3)	85.7540(10)
γ [°]	68.113(3)	70.933(2)
Volume [Å^3]	3551.2(5)	6231.7(3)
Z	1	1
ρ_{calc} [g/cm^3]	1.163	1.506
μ [mm^{-1}]	2.328	7.967
F(000)	1324	2906
Radiation	CuK_α (λ=1.54178 Å)	CuK_α (λ=1.54178 Å)
2θ range [°]	10.33 to 133.19 (0.84 Å)	3.32 to 133.35 (0.84 Å)
Index ranges	$-18 \le h \le 18$ $-19 \le k \le 19$ $-19 \le l \le 19$	$-17 \le h \le 17$ $-19 \le k \le 19$ $-32 \le l \le 31$
Reflections collected	32267	78257
Independent reflections	12401 R_{int} = 0.0359 R_{sigma} = 0.0388	21883 R_{int} = 0.0460 R_{sigma} = 0.0418
Completeness to θ = 66.561°	98.8 %	99.2 %
Data / Restraints / Parameters	12401/198/868	21883/391/1617
Goodness-of-fit on F^2	1.080	1.022
Final R indexes [$I \ge 2\sigma(I)$]	R_1 = 0.0513 wR_2 = 0.1505	R_1 = 0.0491 wR_2 = 0.1402
Final R indexes [all data]	R_1 = 0.0558 wR_2 = 0.1548	R_1 = 0.0546 wR_2 = 0.1441
Largest peak/hole [e/Å^3]	1.06/-0.53	1.43/−1.29

Table S3. Selected bond lengths (Å) for **Ti4-TBC6A** and **Ti28-TBC6A**.

Ti4-TBC6A			
Atom-Atom	**Length / Å**	**Atom-Atom**	**Length / Å**
Ti1–O1$^{\#1}$	2.0171(16)	Ti2–O1	1.9429(15)
Ti1–O1	1.8938(15)	Ti2–O2	1.8091(17)
Ti1–O4	1.8214(16)	Ti2–O3	1.8765(15)
Ti1–O5	1.9962(15)	Ti2–O5$^{\#1}$	2.0476(16)
Ti1–O6	1.8050(16)	Ti2–O7	1.7772(16)
Ti1–N1	2.304(2)		
Ti28-TBC6A			
Atom-Atom	**Length / Å**	**Atom-Atom**	**Length / Å**
Ti1–O37	1.938(2)	Ti8–O51	1.914(2)
Ti1–O2	2.019(2)	Ti8–O52	1.830(2)
Ti1–O39	1.929(2)	Ti8–O58	1.858(2)
Ti1–O5$^{\#1}$	2.125(2)	Ti8–O14	2.057(3)
Ti1–O38	1.770(2)	Ti8–O32	2.058(3)
Ti1–O20	2.012(2)	Ti8–O31	2.070(3)
Ti2–O37	1.902(2)	Ti9–O54	1.965(2)
Ti2–O40	1.973(2)	Ti9–O55	1.960(2)
Ti2–O41	1.809(3)	Ti9–O56	1.743(3)
Ti2–O7	1.997(3)	Ti9–O58	2.169(2)
Ti2–O10	2.028(3)	Ti9–O29	2.015(3)
Ti2–O8	2.050(3)	Ti9–O15	2.015(3)
Ti3–O51	2.024(2)	Ti10–O54	1.989(3)
Ti3–O40	2.052(2)	Ti10–O45	1.764(2)
Ti3–O41	1.829(2)	Ti10–O58	1.906(2)
Ti3–O39	1.878(2)	Ti10–O28	2.129(3)
Ti3–O35	1.984(3)	Ti10–O30	2.015(3)
Ti3–O33	2.003(3)	Ti10–O57	2.010(3)
Ti4–O42	1.889(2)	Ti11–O43	1.885(3)
Ti4–O40	1.890(2)	Ti11–O46	1.899(3)
Ti4–O52	1.840(2)	Ti11–O47	1.848(3)
Ti4–O11	2.069(3)	Ti11–O24	2.089(3)
Ti4–O12	2.055(3)	Ti11–O19	2.013(3)
Ti4–O9	2.051(3)	Ti11–O22	2.035(3)
Ti5–O42	1.900(2)	Ti12–O54	1.920(3)
Ti5–O43	2.023(2)	Ti12–O46	1.895(3)
Ti5–O53	1.838(2)	Ti12–O47	1.809(3)
Ti5–O38	1.854(2)	Ti12–O25	2.047(3)
Ti5–O17	2.099(3)	Ti12–O26	2.072(3)
Ti5–O18	2.059(3)	Ti12–O48	2.043(3)
Ti6–O51	1.977(3)	Ti13–O56	1.920(3)

Ti6–O39	2.045(2)	Ti13–O46	2.049(3)
Ti6–O21	2.017(3)	Ti13–O44	1.918(3)
Ti6–O53	1.776(2)	Ti13–O23	2.052(3)
Ti6–O45	1.866(2)	Ti13–O36	1.771(3)
Ti6–O34	2.135(3)	Ti13–O27	2.049(3)
Ti7–O42	2.217(2)	Ti14–O37$^{\#1}$	2.016(2)
Ti7–O43	1.944(2)	Ti14–O2$^{\#1}$	2.012(2)
Ti7–O55	1.974(3)	Ti14–O1$^{\#1}$	1.828(2)
Ti7–O44	1.726(2)	Ti14–O6$^{\#1}$	2.019(2)
Ti7–O16	2.014(3)	Ti14–O3	1.802(2)
Ti7–O13	1.991(3)	Ti14–O4	2.084(2)

Symmetry transformations used to generate equivalent atoms: #1: 1-X, 2-Y, 1-Z.

Table S4. A summary of calix[n]arene functionalized TOCs.

Formula	Type of calix[n]arene	Number of calix[n]arene	Number of Ti atom	Refs.
$[Ti_2(TBC4A)_2(^nBuO)_2]$	TBC4A	2	2	[6]
$[Ti_4(TC4A)(^nBuO)_8(^iPrO)_4]$	TC4A	1	4	[7]
$[Ti_6O_3(TC4A)(ox)(^iPrO)_{12}]$	TC4A	1	6	[7]
$[Ti_{12}O_4(PgC3)(^iPrO)_{28}]$	PgC3	1	12	[8]
$[Ti_{13}O_{14}(TBC4A)_6]$	TBC4A	6	13	[8]
$[Ti_{12}(TBC4A)_6(Pdc)_6(^iPrO)_{12}]$	TBC4A	6	12	[9]
$[Ti_{12}(TBC4A)_6(Pip)_6(^iPrO)_{12}]$	TBC4A	6	12	[9]
$[Ti_{16}O_8(C4A)_4(PO_4)_4(^iPrO)_{20}(HO^iPr)]$	C4A	4	16	[10]
$[Ti_6O_2(TBC6A)(BA)_4(^iPrO)_{10}]$	TBC6A	1	6	[11]
$[Ti_8(TBC6A)_2(Sal)_4(EtO)_{14}]$	TBC6A	2	8	[11]
$[Ti_4O(TBC6A)(CH_3O)_9]$	TBC6A	1	4	[12]
$[Ti_8O_4(H3TBC6A)_4(C_6H_5PO_3)_8]$	TBC6A	4	8	[13]
$[H_4Ti_{16}O_8(TBC8A)_4(ox)_4(Ac)_4(^iPrO)_8]$	TBC8A	4	16	[14]
$[Ti_4O_2(C8A)(^iPrO)_4(^iPrOH)]$	C8A	1	4	[15]
$[Ti_7O_4(C8A)(CH_3O)_{12}]$	C8A	1	7	[15]
$[Ti_{10}O_3(TBC8A)(OOCC_6F_5)_{12}(^iPrO)_6]$	TBC8A	1	10	[16]
$[Ti_4O_2(TBC6A)_2(CH_3CN)_2]$	**TBC6A**	**2**	**4**	**This work**
$[Ti_{28}O_{36}(TBC6A)(PA)_{34}(^iPrO)_2]$	**TBC6A**	**1**	**28**	**This work**

Abbreviations: TBC4A = tert-butylcalix[4]arene; TC4A = *p*-tert-Butylthiacalix[4]arene; C4A = calix[4]arene; TBC6A = tert-butylcalix[6]arene; TBC8A = tert-butylcalix[8]arene; PgC3 = C-propylpyrogallol[4]arene; H_2Pdc = pyridine-3,5-dicarboxylic acid; H_2pip = 5-(pyridin-4-yl)isophthalic acid; BA = benzoic acid; Sal = salicylic acid; PA = propionic acid; ox = Oxalic acid.

Table S5. A summary of the catalytic performance of various reported photocatalysts for the cycloaddition reactions of CO_2 and epoxides.

Catalyst	Condition	Cocatalsyt	Time (h)	Conversion (%)	Ref.
$Ti_{18}Bi_{14}$	Catalyst (100 mg), 300W xenon lamp, *r.t.*	TBAB	14	99	[17]
Bi-PCN-224	Catalyst (30 mg), 300W xenon lamp, *r.t.*	TBAB	6	99	[18]
PMo_{12}@Zr-Fc MOF	Catalyst (5 mg), simulated sunlight 0.5W cm^{-2}, 90 °C	TBAB	8	90	[19]
HPC-800	Catalyst (30 mg), 300mW cm^{-2} full-spectrum irradiation, *r.t.*	TBAB	10	94	[20]
Co2C nanoflowers	Catalyst (25 mg), blue LEDs 450 nm, 60 °C	TBAB	15	93.5	[21]
Al-N-C	Catalyst (20 mg), 400mW cm^{-2} full-spectrum Irradiation, *r.t.*	TBAB	36	95	[22]
$PC_{61}BM$/CuTCPP-1.8%	Catalyst (1 mg), 100mW cm^{-2} Xeon lamp (400 nm < λ < 800 nm), *r.t.*	TBAB	60	92.4	[23]
$Ti_{10}Pb_2$	Catalyst (100 mg), simulated solar irradiation, *r.t.*	TBAB	26	98	[24]
OH-P[5]-on-COF	Catalyst (1.5 g), 300W xenon lamp, *r.t.*	TBAB	3	99	[25]
$W_{18}O_{49}$/g-C_3N_4	Catalyst (30 mg), 300W Xe lamp, *r.t.*	TBAB	4	78	[26]
$Ti_{12}Cs$	Catalyst (100 mg), simulated solar irradiation, *r.t.*	TBAB	8	98	[27]
Ti28-TBC6A	**Catalyst (15 mg), 10W 430 nm LED, *r.t.***	**TBAB**	**20**	**96**	**This work**

References

1 J. P. Perdew, K. Burke, M. Ernzerhof, Generalized Gradient Approximation Made Simple. *J. Phys. Rev. Lett.*, 1996, **77**, 3865−3868.

2 B. Delley, An All-Electron Numerical Method for Solving the Local Density Functional for Polyatomic Molecules. *J. Chem. Phys.*, 1990, **92**, 508−517.

3 B. Delley, From Molecules to Solids with the Approach. *J. Chem. Phys.*, 2000, **113**, 7756−7764.

4 S. Grimme, Semiempirical GGA-Type Density Functional Constructed with a Long-Range Dispersion Correction. *J. Comput. Chem.*, 2006, **27**, 1787−1799.

5 I. D. Brown, Recent Developments in the Methods and Applications of the Bond Valence Model, *Chem. Rev.*, 2009, **109**, 6858-6919.

6 M. Czakler, C. Artner, C. Maurer and U. Schubert, Calix[4]arene derivatives of titanium and zirconium alkoxides, *Zeitschrift für Naturforschung B*, 2014, **69**, 1253-1259.

7 X. Wang, Y. Yu, Z. Wang, J. Zheng, Y. Bi and Z. Zheng, Thiacalix[4]arene-Protected Titanium–Oxo Clusters: Influence of Ligand Conformation and Ti–S Coordination on the Visible-Light Photocatalytic Hydrogen Production, *Inorg. Chem.*, 2020, **59**, 7150-7157.

8 K. Su, M. Wu, Y. Tan, W. Wang, D. Yuan and M. Hong, A monomeric bowl-like pyrogallol[4]arene Ti_{12} coordination complex, *Chem. Commun.*, 2017, **53**, 9598-9601.

9 Y.-Q. Tian, Y.-S. Cui, J.-H. Zhu, C.-Q. Xu, X.-Y. Yi, J. Li and C. Liu, Ancillary ligand-regulated Ti(iv)-based metallocalixarene coordination cages for photocatalytic H_2 evolution, *Chem. Commun.*, 2022, **58**, 9034-9037.

10 N. Li, J.-M. Lin, R.-H. Li, J.-W. Shi, L.-Z. Dong, J. Liu, J. He and Y.-Q. Lan, Calix[4]arene-Functionalized Titanium-Oxo Compounds for Perceiving Differences in Catalytic Reactivity Between Mono-and Multimetallic Sites, *J. Am. Chem. Soc.*, 2023, **145**, 16098-16108.

11 L.-F. Dai, X.-R. Liu, Y.-Q. Tian, X.-Y. Yi and C. Liu, Auxiliary Carboxylate-Induced Assembly of Calix[6]arene-Polyoxotitanate Hybrid Systems with Photocatalytic Activity in the Oxidation of Sulfides, *Inorg. Chem.*, 2023, **62**, 6047-6054.

12 C. Wang, S.-J. Wang and F.-G. Kong, Calixarene-protected titanium-oxo clusters and their photocurrent responses and photocatalytic performances, *Inorg. Chem.*, 2021, **60**, 5034-5041.

13 Y. Wang, H. Zheng, G. Zhang, H. Wang, Y. Xiong and W. Liao, Solvent-Polarity-Induced Assembly of Calixarene-Capped Titanium-Oxo Clusters with Catalytic Activity in the Oxygenation of Sulfides, *Eur. J. Inorg. Chem.*, 2023, **26**, e202200677.

14 Y.-Q. Tian, L.-F. Dai, W.-L. Mu, W.-D. Yu, J. Yan and C. Liu, Atomically accurate site-specific ligand tailoring of highly acid-and alkali-resistant Ti(iv)-based metallamacrocycle for enhanced CO_2 photoreduction, *Chem. Sci.*, 2023, **14**, 14280-14289.

15 N. Li, J.-J. Liu, J.-W. Sun, B.-X. Dong, L.-Z. Dong, S.-J. Yao, Z. Xin, S.-L. Li and Y.-Q. Lan, Calix[8]arene-constructed stable polyoxo-titanium clusters for efficient CO_2 photoreduction, *Green Chem.*, 2020, **22**, 5325-5332.

16 X.-X. Yang, W.-D. Yu, X.-Y. Yi, L.-J. Li and C. Liu, Monocarboxylate-driven structural growth in Calix[n]arene-polyoxotitanate hybrid systems: utility in hydrogen production from water, *Chem. Commun.*, 2020, **56**, 14035-14038.

17 C. Liu, H. Niu, D. Wang, C. Gao, A. Said, Y. Liu, G. Wang, C.-H. Tung and Y. Wang, S-scheme Bi-oxide/Ti-oxide molecular hybrid for photocatalytic cycloaddition of carbon dioxide to epoxides, *ACS Catal.*, 2022, **12**, 8202-8213.

18 G. Zhai, Y. Liu, L. Lei, J. Wang, Z. Wang, Z. Zheng, P. Wang, H. Cheng, Y. Dai and B. Huang, Light-promoted CO_2 conversion from epoxides to cyclic carbonates at ambient conditions over a Bi-based metal–organic framework, *Acs Catal.*, 2021, **11**, 1988-1994.

19 Z. Fang, Z. Deng, X. Wan, Z. Li, X. Ma, S. Hussain, Z. Ye and X. Peng, Keggin-type polyoxometalates molecularly loaded in Zr-ferrocene metal organic framework nanosheets for solar-driven CO_2 cycloaddition, *Appl. Catal. B Environ.*, 2021, **296**, 120329.

20 Q. Yang, C. C. Yang, C. H. Lin and H. L. Jiang, Metal–organic-framework-derived hollow N-doped porous carbon with ultrahigh concentrations of single Zn atoms for efficient carbon dioxide conversion, *Angew. Chem. Int. Ed.,* 2019, **131**, 3549-3553.

21 Q. Guo, S.-G. Xia, X.-B. Li, Y. Wang, F. Liang, Z.-S. Lin, C.-H. Tung and L.-Z. Wu, Flower-like cobalt carbide for efficient carbon dioxide conversion, *Chem. Commun.*, 2020, **56**, 7849-7852.

22 Q. Yang, H. Peng, Q. Zhang, X. Qian, X. Chen, X. Tang, S. Dai, J. Zhao, K. Jiang and Q. Yang, Atomically dispersed high-density Al–N4 sites in porous carbon for efficient photodriven CO_2 cycloaddition, *Adv. Mater.*, 2021, **33**, 2103186.

23 Y. Guo, B. Gao, Z. Deng, Y. Liu, X. Peng and Y. Zhao, Charge separation in hybrid metal–organic framework films for enhanced catalytic CO_2 conversion, *J. Mater. Chem. A*, 2021, **9**, 2694-2699.

24 A. Said, G. Zhang, C. Liu, D. Wang, H. Niu, Y. Liu, G. Chen, C.-H. Tung and Y. Wang, A butterfly-like lead-doped titanium-oxide compound with high performance in photocatalytic cycloaddition of CO_2 to epoxide, *Dalton Trans.*, 2023, **52**, 2392-2403.

25 X. Li, X. Niu, P. Fu, Y. Song, E. Zhang, Y. Dang, J. Yan, G. Feng, S. Lei and W. Hu, Macrocycle-on-COF photocatalyst constructed by in-situ linker exchange for efficient photocatalytic CO_2 cycloaddition, *Appl. Catal. B Environ.*, 2024, **350**, 123943.

26 R. Cheng, A. Wang, S. Sang, H. Liang, S. Liu and P. Tsiakaras, Photocatalytic CO_2 cycloaddition over highly efficient $W_{18}O_{49}$-based composites: An economic and ecofriendly choice, *Chem. Eng. J.*, 2023, **466**, 142982.

27 Y. Liu, G. Zhang, D. Wang, G. Chen, F. Gao, C.-H. Tung and Y. Wang, A cryptand-like Ti-coordination compound with visible-light photocatalytic activity in CO_2 storage, *Dalton Trans.*, 2024, **53**, 1989-1998.